Quantitation of Human Metallothionein Isoforms: A Family of Small, Highly Conserved, Cysteine-rich Proteins*[S]

Aaron A. Mehus‡§¶, Wallace W. Muhonen‡, Scott H. Garrett§, Seema Somji§, Donald A. Sens§, and John B. Shabb‡‖

Human metallothioneins (MTs) are important regulators of metal homeostasis and protectors against oxidative damage. Their altered mRNA expression has been correlated with metal toxicity and a variety of cancers. Current immunodetection methods lack the specificity to distinguish all 12 human isoforms. Each, however, can be distinguished by the mass of its acetylated, cysteine-rich, hydrophilic N-terminal tryptic peptides. These properties were exploited to develop a bottom-up MALDI-TOF/TOF-MS-based method for their simultaneous quantitation. Key features included enrichment of N-terminal acetylated peptides by strong cation exchange chromatography, optimization of C18 reversed-phase chromatography, and control of methionine oxidation. Combinations of nine isoforms were identified in seven cell lines and two tissues. Relative quantitation was accomplished by comparing peak intensities of peptides generated from pooled cytosolic proteins alkylated with ^{14}N- or ^{15}N-iodoacetamide. Absolute quantitation was achieved using ^{15}N-iodoacetamide-labeled synthetic peptides as internal standards. The method was applied to the cadmium induction of MTs in human kidney HK-2 epithelial cells expressing recombinant MT-3. Seven isoforms were detected with abundances spanning almost 2 orders of magnitude and inductions up to 12-fold. The protein-to-mRNA ratio for MT-1E was one-tenth that of other MTs, suggesting isoform-specific differences in protein expression efficiency. Differential expression of MT-1G1 and MT-1G2 suggested tissue- and cell-specific alternative splicing for the MT-1G isoform. Protein expression of MT isoforms was also evaluated in human breast epithelial cancer cell lines. Estrogen-receptor-positive cell lines expressed only MT-2 and MT-1X, whereas estrogen-receptor-negative cell lines additionally expressed MT-1E. The combined expression of MT isoforms was 38-fold greater in estrogen-receptor-negative cell lines than in estrogen-receptor-positive cells. These findings demonstrate that individual human MT isoforms can be accurately quantified in cells and tissues at the protein level, complementing and expanding mRNA measurement as a means for evaluating MTs as potential biomarkers for cancers or heavy metal toxicity. ***Molecular & Cellular Proteomics 13: 10.1074/mcp.M113.033373, 1020–1033, 2014.***

The metallothioneins (MTs)[1] are a family of small, highly conserved proteins with the specific capacity to bind metal ions (1–3). Mammalian MTs, typically 61 to 68 amino acid residues in length, contain 20 invariant cysteine residues that form two distinct metal-binding domains. Up to seven or eight metal ions may be coordinated per MT. Many functions have been attributed to this redox-active protein, including zinc homeostasis; heavy metal detoxification; metal exchange; metal transfer; and protection against oxidative damage, inflammatory responses, and other cellular stresses (4–6). Changes in MT expression have been associated with human pathologies including cadmium-induced renal toxicity (7), neurodegeneration (8), and many forms of cancer (9, 10). The understanding of these changes is complicated by the 11 functional MT genes, seven pseudogenes, and four MT-like genes encoded in the genome, most of which contain only small differences in amino acid sequence (11). Seventeen of the 18 genes and pseudogenes are clustered together on chromosome 16, which is known to be enriched for intrachromosomal duplications (12). The various MT gene products differ in their patterns of mRNA and protein expression in human tissues and cell lines. Immunohistochemical detection using antibodies that do not discriminate between MT-1 and MT-2 isoforms indicates wide tissue and cell type distribution of MTs, as illustrated with the MT-1A entry of the Human Protein Atlas (13, 14). Measurements of individual MT mRNA

From the ‡Department of Basic Sciences, School of Medicine and Health Sciences, University of North Dakota, 501 Columbia Road N., Grand Forks, North Dakota 58203; §Department of Pathology, School of Medicine and Health Sciences, University of North Dakota, 501 Columbia Road N., Grand Forks, North Dakota 58203

Received August 10, 2013, and in revised form, January 9, 2014
Published, MCP Papers in Press, February 3, 2014, DOI 10.1074/mcp.M113.033373
Author contributions: A.A.M., S.H.G., S.S., D.A.S., and J.B.S. designed research; A.A.M. and W.W.M. performed research; W.W.M., S.H.G., S.S., and D.A.S. contributed new reagents or analytic tools; A.A.M. and J.B.S. analyzed data; A.A.M. and J.B.S. wrote the paper.

[1] The abbreviations used are: MT, metallothionein; ER$^+$, estrogen-receptor positive; ER$^-$, estrogen-receptor negative; RP-HPLC, reversed-phase high-pressure liquid chromatography; SCX, strong cation exchange.

levels, however, clearly demonstrate differential expression of specific MT-1 isoforms in human tissues and cell lines (15–17). The MT-3 (18, 19) and MT-4 (20) mRNAs are expressed in even narrower ranges of cell types.

An abundance of immunohistochemical and mRNA measurements show that alteration of MT isoform expression is correlated with a variety of cancers (9, 10). For example, several studies show that the expression of specific MT isoforms is altered in invasive ductal breast carcinomas. Elevated MT-2A (21) or MT-1F (22) is correlated with increased proliferation or tumor grade, respectively. Expression of MT-3 is associated with poor prognosis (23, 24). The MT-1E isoform is found in estrogen-receptor-negative (ER^-), but not estrogen-receptor-positive (ER^+), tumors (25) and cell lines (26). Parallel assessment of changes in MT protein expression via immunohistochemistry supports the mRNA data up to a point. Except for antibodies specific for the MT-3 isoform (27), all commercially available MT antibodies are pan-specific for the MT-1, MT-2, and MT-4 protein isoforms (28). This is because epitopes recognized by antibodies raised against MT-1 or MT-2 are limited to the first five residues of the acetylated N terminus, which are invariant among all MT-1, MT-2, and MT-4 isoforms (29–31). This includes the commercially available E9 antibody that has been used to demonstrate the overexpression of MT in a wide variety of human cancers (28, 32, 33). In general, the overexpression of MT in various cancers has been associated with resistance to anticancer therapies and linked to a poor prognosis.

The mounting evidence that specific MT isoforms may be useful prognostic and diagnostic markers for cancers highlights the need for alternative approaches to the assessment of MT isoform expression at the protein level. A few mass-spectrometry-based studies have succeeded in identifying the complement of MT isoforms in human cells (34, 35). Though top-down approaches hold promise for the quantitation of MTs based on the unique masses of intact isoforms (34, 36), this has yet to be exploited. Inductively coupled plasma MS has been used to quantify total metal-bound MTs in cells and tissues, but it cannot assign relative abundance values of MT isoforms because the proteins are reduced to their elemental composition with this technique. Thus far, MALDI-MS has been used in parallel with inductively coupled plasma MS for the qualitative identification of isoforms (35). Bottom-up quantitative approaches specifically targeting MTs have not yet been reported.

The use of mass spectrometry to quantify MT isoforms is not straightforward. The N-terminal tryptic peptide of each human MT isoform encompasses the only sequence that distinguishes all 12 and therefore may be used for their identification and quantitation in complex biological samples from cells and tissues (34). Any attempt at quantitation of this family of small, highly conserved, cysteine-rich proteins therefore requires reproducible detection of these signature peptides.

An optimized bottom-up proteomic method is presented here that is capable of identifying and quantifying all isoforms that constitute the human MT gene family in a single experiment. The approach is comparable in sensitivity and dynamic range to quantitative PCR methods used to measure mRNA levels. Quantitative and qualitative differences between mRNA and protein expression indicate that isoform-specific measurements of protein levels complement and extend our understanding of MT isoform expression in complex biological samples. The method was applied to the characterization of MT isoforms in ER^+ and ER^- breast cancer cell lines. Protein and mRNA measurements showed the same complement of isoform expression, confirming differential MT expression between ER^+ and ER^- cell lines. The mass spectrometry assay further showed dramatic differences in the abundance of protein and mRNA in specific isoforms, an observation that has not been previously reported.

EXPERIMENTAL PROCEDURES

Materials and Reagents—^{15}N-iodoacetamide was obtained from Sigma-Aldrich (St. Louis, MO). Isoform-specific N-terminal acetylated MT peptides were synthesized by Elim Biopharmaceuticals (Hayward, CA). All reagents used for protein sample preparation were mass-spectrometry grade when available. Human cerebrum was obtained as an existing biological specimen from the Brain and Tissue Bank for Developmental Tissue Disorders (University of Maryland, Baltimore, MD) and stored at −80 °C. Adult human kidney cortex was obtained as described elsewhere (19, 37) and stored at −80 °C. All procurement protocols were approved by the University of North Dakota Institutional Review Board for Human Research.

Cell Culture and Harvest—Human kidney epithelial HK-2 (MT-3) cells containing stably transfected human MT-3 were grown as described previously (38, 39). This permanent cell line was selected because it mimics the doming properties of primary cultures of human proximal tubule cells. Upon doming of confluent monolayers, cells were maintained for 3 days in the presence or absence of 9 μM $CdCl_2$ to induce MT expression. The human breast cell lines MCF-10A, MCF-7, T-47D, Hs578T, and MDA-MB-231 were obtained from the American Type Culture Collection. The MCF-10A cells were grown as previously described (40, 41) except media were supplemented with 5% (v/v) fetal calf serum. Cell monolayers from two T-75 flasks were washed twice with phosphate-buffered saline, detached by scraping, and pelleted by centrifugation at 197 × *g* for 5 min at 4 °C. Harvested cells were aliquoted for mass spectrometry and PCR analysis and either stored at −80 °C or used immediately.

Cytosol Preparation from Cells—Cell pellets were resuspended in 0.5 ml of hypotonic buffer (10 mM Tris pH 8.0, 1.5 mM $MgCl_2$, 10 mM KCl, 1 mM DTT, and 0.5 μl Protease Inhibitor Mixture (Sigma-Aldrich)). The cells were then passed through a 25-gauge, ⅝-in. needle three times to disrupt membranes. The nuclei were pelleted by centrifugation (800 × *g* for 10 min at 4 °C) and the supernatant was further clarified by centrifugation at 100,000 × *g* for 30 min at 4 °C. Typical yields of 0.5 ml of cytosol per two T-75 flasks were 3.0 to 3.5 mg/ml as determined by the Bio-Rad Protein Assay (Bio-Rad, Hercules, CA). Cytosols were stored at −80 °C.

Cytosol Preparation from Tissues—Approximately 100 mg of frozen tissue was suspended in three volumes of hypotonic buffer and disrupted on ice with a Dounce homogenizer. All subsequent steps were as described for cell cytosol preparations.

Reduction and Alkylation—300 μg of cytosol (~100 μl) was incubated with 3.5 mM EDTA. Samples were then denatured with 8 M urea

and reduced with 5 mM DTT or tris(2-carboxyethyl)phosphine in 100 mM Tris pH 8.0 for one hour at room temperature in a final volume of ~190 μl. Proteins were then alkylated at room temperature in the dark for one hour by the addition of ~27 μl of 200 mM ^{14}N- or ^{15}N-iodoacetamide to a final concentration of 28 mM. Urea and excess alkylating agent were removed by passage through 1 ml of Bio-Gel P-6 in micro-Bio-Spin chromatography columns (Bio-Rad Laboratories, Hercules, CA) equilibrated with 100 mM Tris pH 8.0.

^{15}N-labeled Peptide Standards—Table I shows the sequences for the 12 acetylated N-terminal tryptic peptides from human MTs surveyed in this study. All but MT-1G1 were successfully synthesized. The wide range of peptide purity in samples as received from the manufacturer (supplemental Table S1) was attributed to the difficulty of synthesis related to the high cysteine content and peptide-specific sequences. Peptides with ^{15}N-iodoacetamide-blocked cysteines were not synthesized directly because of the prohibitive cost of doing so. 30 μg (30.0 μl) of each peptide was reduced and alkylated as described above in a final volume of 35.9 μl. The ^{15}N-labeled peptides were then purified via reversed-phase high-pressure liquid chromatography (RP-HPLC) using a narrow-bore 2.1 × 150 mm Zorbax 300SB-C18 5-μm bead-size column (Agilent Technologies, Santa Clara, CA) on a Shimadzu 10-AVP HPLC (Shimadzu, Kyoto, Japan). Peptides were separated with a linear 35-min gradient using 97% buffer A (0.1% formic acid) to 38% buffer B (0.1% formic acid, 90% acetonitrile) at 0.3 ml/min and detected by absorbance at 214 nm. Samples with peaks corresponding to the correct mass and sequence as determined by mass spectrometry (supplemental Fig. S1) were collected, dried, reconstituted in MS-grade water, and stored at −80 °C. At this stage, all ^{15}N-labeled peptides were at least 95% pure as assessed by RP-HPLC. Peptide concentrations were determined by means of area-under-the-curve analysis at 214 nm using the manufacturer's elemental analysis of the MT peptide with the highest initial purity as the reference standard. The fully alkylated peptides were unusually hydrophilic for their sizes, which were between 2220.8 and 2418.8 *m/z* (Table I). Furthermore, the ionization intensities of these peptides were comparable when analyzed in the same experiment (supplemental Table S1). The stock reference mixtures for absolute quantitation were tailored to match endogenous MTs in a given cell line. For HK-2(MT-3) cells, 145 μM each of ^{15}N-labeled peptides MT-2, MT-3, MT-1E, MT-1G2, MT-1X, MT-1M, and MT-1F were used. For the breast cells, 100 μM each of ^{15}N-labeled peptides MT-2, MT-1E, and MT-1X were used.

Trypsin Digestion—For relative quantitation, which was done only for HK-2 cells, 300 μg each of ^{14}N-labeled control cytosol and ^{15}N-labeled Cd^{2+}-treated cytosol were combined. For absolute quantitation, which was done for HK-2 cells and breast cell lines, 1 μl of ^{15}N-labeled MT peptide reference mix was added to 300 μg of ^{14}N-labeled cytosol. Samples were incubated with modified trypsin (2% w/w; Trypsin Gold, Promega, Madison, WI) overnight at 37 °C. The reaction was stopped by the addition of formic acid to a 0.1% final concentration. Peptides were desalted online via HPLC through a self-packed Magic C18AQ column (200-Å pore size, 5-μm-diameter particles; Michrom Bioresources, Auburn, CA) using 0.15 ml/min 0.1% formic acid for 20 min. The peptides were then eluted onto the strong cation exchange (SCX) column using a 500-μl injection of 75% acetonitrile and 0.1% formic acid.

Chromatography—Peptides were fractionated on a self-packed 2.1 mm by 25 cm poly LC polysulfoethyl A (SCX) analytical column equilibrated with 0.1% formic acid and eluted with a 60-min linear gradient to 25% buffer containing 0.1% formic acid, 1 M NaCl, and 10% acetonitrile at 0.15 ml/min. Fractions were collected every 7 min and screened by mass spectrometry to locate the MT peptides. The MT-peptide-containing fraction was evaporated to dryness and reconstituted in 24 μl of 8 M HCl containing 0.5 M dimethyl sulfide. The reaction was incubated for 30 min at room temperature to reduce methionine sulfoxides (42). The reaction was then quenched by the addition of 12 μl of 5 M NaOH. Precipitated salt was pelleted by centrifugation at 14,000 × *g* for 2 min at room temperature and the supernatant was collected. The sample was immediately loaded onto a self-packed 100 μm by 10 cm Magic C18AQ column using a Tempo LC-MALDI (AB SCIEX, Framingham, MA) integrated nano-HPLC/spotter. The column was equilibrated with 97% buffer A (0.1% formic acid, 2% acetonitrile) and 3% buffer B (0.1% formic acid, 98% acetonitrile) at a flow rate of 0.8 μl/min, and peptides were fractionated with a 70-min linear gradient of 3% buffer B/97% buffer A to 20% buffer B/80% buffer A. Fractions were spotted every 18 s onto a MALDI target plate with post-column mixing of an equal volume of 10 mg/ml α-cyano-4-hydroxycinnamic acid in 75% acetonitrile, 0.1% formic acid. The column was recycled with 70% buffer B/30% buffer A for 5 min and then re-equilibrated with 3% buffer B for 10 min.

Mass Spectrometry—The samples were analyzed via MS and MS/MS using an AB SCIEX 4800 MALDI-TOF/TOF mass spectrometer. For MS, the laser intensity was 3200 to 3500 and spectra were accumulated over 30 subspectra at 30 shots per subspectrum. The precursor ion mass range was limited to *m/z* 1800–3000. The resolution was typically 15,000. For MS/MS, the laser intensity was 4000, and spectra were accumulated over 30 subspectra at 30 shots per subspectrum. Unprocessed .t2d files were centroided and converted to .mgf files using the Peaks to Mascot tool in the AB Sciex 4000 Explorer software (version 3.5.28193). MT peptides were identified using Mascot version 2.3.02 (Matrix Science Inc., Boston, MA). Spectra were searched against the human proteome (34,765 sequences) in the UniProt protein database (version 15.15). False discovery rates were not determined, as the objective of the database search was to confirm the identities of a handful of well-characterized peptides. The peptide mass tolerance was 1.2 Da, and the fragment ion tolerance was 0.6 Da. The enzyme was set as trypsin with up to two missed cleavages. Cysteine ^{15}N-carbamidomethylation was allowed as a fixed modification. Variable modifications were acetylation (protein N-term), methionine oxidation, and cysteine ^{14}N-carbamidomethylation. The use of ^{14}N- and ^{15}N-carbamidomethylation in this combination permitted the identification of either ^{14}N-labeled or ^{15}N-labeled MT peptides in a single search. Peptide mass errors were typically less than 100 ppm. Mascot ion scores were routinely between 60 and 150 for MT peptides. Annotated spectra were graphically represented using Scaffold v.3 (Proteome Software, Portland, OR).

Relative and Absolute Quantitation—The mean monoisotopic peak intensity was determined for each ^{14}N- and ^{15}N-labeled MT peptide precursor ion across three to five spots spanning the precursor ion peak. The minimum signal-to-noise ratio accepted for a given peak was 20. The mass difference between pairs of ^{14}N- and ^{15}N-labeled MT precursor ion pairs was 5 Da. Intensities of the ^{15}N-labeled monoisotopic peaks were corrected for the contribution of the overlapping ^{14}N peptide $n + 6$ isotopic peak using the equation $H_{corr} = H - L \times C - P \times (H - L \times C)$, where H and L are the areas of the monoisotopic peaks of the ^{15}N- and ^{14}N-labeled precursor ions, respectively, C is the fractional contribution of the ^{14}N-labeled precursor ion $n + 6$ isotopic peak calculated using MS-Isotope (Protein Prospector), and P is the fractional atom percent of ^{14}N in ^{15}N iodoacetamide (0.01 according to the manufacturer).

Real-time Analysis of MT Isoform mRNA Expression—Total RNA was purified from cell pellets using the manufacturer's standard TRI Reagent (Molecular Research Center, Cincinnati, OH) protocol. Real time RT-PCR measurement of MT mRNA expression was done according to Ref. 43 utilizing previously described MT isoform-specific primers (37), except for MT-1M. The MT-1M primers were sense GGGCCTAGCAGTCG and antisense TGGCTCAGTATCGTATTG with a product size of 322 base pairs. The primer sequences used for 18S

TABLE I

Identification of acetylated N-terminal MT peptides in human cell lines and tissues. Human MT isoforms were identified via mass spectrometry based on their unique N-terminal tryptic peptides. Masses of singly protonated precursor ions (MH^{1+}) include N-terminal acetylation and carbamidomethylation of Cys residues. Experimental masses (not shown) were consistently within 50 ppm of the expected m/z. Retention times are based on optimized RP-HPLC and are given to indicate the relative order of MT peptide elution. Mascot ion scores represent the highest scoring MS/MS spectrum for each peptide from ^{15}N-labeled synthetic peptides and ^{14}N-labeled endogenous peptides (see supplemental Figs. S1 and S2). Breast ER^+ cell lines are MCF-7 and T-47D. Breast ER^- cell lines are MCF-10A, Hs578T, and MDA-MB-231. The MT-1G1 and MT-1G2 isoforms are splice variants of the MT1G gene. The UniProt database lists the MT-1M sequence shown here as a natural variant that differs by a single Thr-to-Lys transition at position 20. The sequences are aligned to illustrate single amino acid insertions in MT1-G1 and MT-3. Red residues differ from the consensus sequence. Isoform identification was consistent across at least three biological replicates for each cell line or group of cell lines. Tissue identifications were consistent across at least three independent measurements from a single biological specimen

UniProt Accession	MT Isoform	Acetylated N-terminal tryptic peptide	MH^{1+} (m/z)	Retention (min)	Mascot ion score		Cell lines					Tissues	
					synth. (^{15}N)	endog. (^{14}N)	HK-2 (MT3) $-Cd^{2+}$	HK-2 (MT3) $+Cd^{2+}$	ER^+ breast cells	ER^- breast cells	RWPE	Kidney cortex	Brain
P04731	MT-1A	MDPN-CSCAT-GGSCTCTGSCK	2252.78	36.5	142	ND	No	No	No	No	No	No	No
P07438	MT-1B	MDPN-CSCTT-GGSCACAGSCK	2222.77	36.5	163	ND	No	No	No	No	No	No	No
P04732	MT-1E	MDPN-CSCAT-GGSCTCAGSCK	2222.77	37	128	163	Yes	Yes	No	Yes	Yes	Yes	Yes
P04733	MT-1F	MDPN-CSCAA-GVSCTCAGSCK	2234.81	46.9	128	142	Yes	Yes	No	No	Yes	Yes	Yes
P13640	MT-1G1	MDPN-CSCAAAGVSCTCASSCK	2335.85	48.2	ND	140	No	No	No	No	Yes	Yes	Yes
P13640-2	MT-1G2	MDPN-CSCAA-GVSCTCASSCK	2264.82	47.2	134	142	Yes	Yes	No	No	Yes	Yes	Yes
P80294	MT-1H	MDPN-CSCEA-GGSCACAGSCK	2220.75	38.3	141	144	No	No	No	No	No	Yes	No
Q93083	MT-1L	MDPN-CSCAT-GGSCSCASSCK	2238.76	35.8	143	ND	No	No	No	No	No	No	No
Q8N339	MT-1M	MDPN-CSCTT-GVSCACTGSCK	2555.91	45.8	156	156	No	Yes	No	No	Yes	No	No
P80297	MT-1X	MDPN-CSCSP-VGSCACAGSCK	2246.81	48.4	142	142	Yes	Yes	Yes	Yes	Yes	Yes	Yes
P02795	MT-2	MDPN-CSCAA-GDSCTCAGSCK	2250.76	38.5	142	157	Yes	Yes	Yes	Yes	Yes	Yes	Yes
P25713	MT-3	MDPETCPCPS-GGSCTCADSCK	2418.84	45.1	109	89	Yes	Yes	No	No	No	No	Yes

rRNA expression were sense CGCCGCTAGAGGTGAAATTC and antisense TTGGCAAATGCTTTCGCTC with a product size of 62 base pairs. Cycling parameters for 18S rRNA and all MT isoforms except MT-1M consisted of a reverse-transcription step at 50 °C for 10 min, denaturation at 95 °C for 15 s, annealing at 65 °C for 40 s, and extension at 72 °C for 40 s. Parameters for MT-1M were identical, except that 62 °C was used as the annealing temperature.

Statistical Analysis—All results from cell lines are reported as the mean ± S.D. of three biological replicates. The mean coefficient of variance (cv) was 0.19 for all reported mass-spectrometry-based results. The mean cv was 0.26 for all reported real-time PCR measurements. Variation across three technical replicates for each of 19 independent mass-spectrometry-based measurements gave a mean cv of 0.11. Significant differences of $p < 0.05$ were determined with GraphPad Prism 6 using statistical treatments appropriate for the type of experiment as described in the figure legends.

RESULTS

Identification of Endogenous N-terminal MT Peptides—The purpose of this study was to develop a robust mass-spectrometry-based method for quantifying human MT isoforms to complement mRNA-based studies that implicate MTs as potential biomarkers for specific diseases. One-dimensional RP-HPLC was optimized to reproducibly capture the large, hydrophilic, acetylated N-terminal tryptic peptides of human MT isoforms. This method, as described under "Experimental Procedures," was applied for the identification of MT isoforms in Cd^{2+}-induced HK-2(MT3) human kidney epithelial cell cytosol. Seven MT isoforms were identified (Table I) and confirmed by MS/MS (supplemental Figs. S2*A*, S2*B*, S2*D*, and S2*F*–S2*I*). The heat map shown in Fig. 1*A* shows that this one-dimensional separation was sufficient to segregate the MT peptides from the typical smaller early-eluting and larger more hydrophobic tryptic peptides. A second chromatogra-

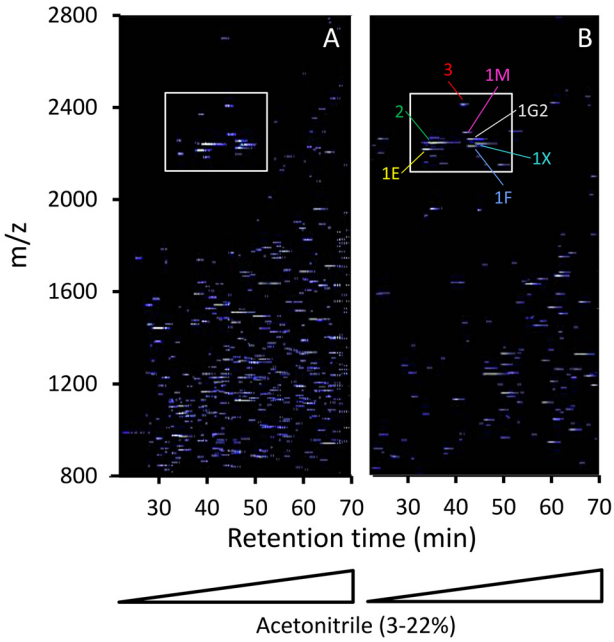

FIG. 1. **Metallothionein N-terminal peptides cluster as a distinct group during one- and two-dimensional LC-MS.** Heat maps show the retention time and mass-to-charge ratio of precursor ions detected by RP-HPLC followed by MALDI-TOF mass spectrometry as described under "Experimental Procedures." *A*, one-dimensional chromatography in which unfractionated tryptic peptides from Cd^{2+}-induced HK-2(MT3) cell cytosol were applied directly to the C18 column. *B*, two-dimensional chromatography in which N-terminal MT peptides were fractionated by SCX chromatography and then the early-eluting MT peptide-containing fraction was applied to the C18 column. The boxed precursor ions are the MT peptides. The most intense ions in this region are fully alkylated and N-terminally acetylated, and their methionine residues are unoxidized.

phy step was introduced to reduce sample complexity and improve sampling depth. SCX chromatography effectively separated the weakly binding MT peptides from the bulk of tryptic peptides (supplemental Fig. S3). This result was consistent with the general SCX fractionation pattern of N-terminally acetylated peptides (44). Fig. 1*B* shows a heat map of the RP-HPLC of the SCX fraction containing MT peptides. It illustrates the high degree of enrichment of the MT peptides achieved with this orthogonal fractionation strategy (boxed area). This two-dimensional approach was critical to increasing the sensitivity of MT-peptide detection in HK-2(MT3) cells that had not been exposed to heavy metal. Only three isoforms (MT-1E, MT1-X, and MT-2) were detected in these uninduced cells by means of RP-HPLC alone, and their signals were very weak (not shown). Using the two-dimensional approach, six of the seven MT isoforms originally detected in Cd^{2+}-induced cells were also detected in uninduced cells (Table I). Increasing the starting amount of cytosol from 300 μg to 800 μg did not produce additional detections of N-terminal MT peptides (data not shown).

The complement of expressed MT isoforms was surveyed in other human cell lines and tissues (Table I). Each tissue or cell type had a unique MT isoform fingerprint. Kidney cortex, cerebrum, and the RWPE prostate cell line each expressed seven isoforms. Notably, both MT-1G splice isoforms, MT-1G1 and MT-1G2, were expressed in kidney, brain, and RWPE cells, whereas only MT-1G2 was detected in HK-2(MT3) cells. The MT-1M isoform was not detected in kidney or brain, compared with HK-2 and RWPE cells. Kidney was the only tissue or cell type that expressed MT-1H, and brain was the only one that expressed endogenous MT-3. The MT profile of breast epithelial cells was more restricted. The ER^- breast epithelial cell lines expressed MT-2, MT-1X, and MT-1E, whereas ER^+ breast epithelial cell lines expressed only MT-2 and MT-1X. Cumulatively, 9 of the 12 MT isoforms were detected in at least one tissue or cell type. The MS/MS results of these endogenous peptides are shown collectively in supplemental Fig. S2. Isoforms not detected included MT-1A, MT-1B, and MT-1L.

N-terminal Modifications of Endogenous MTs—Nearly all N-terminal peptides from endogenous MTs were N-terminally acetylated. A small amount of unmodified MT-2 (10% or less of total MT-2 signal; not shown) was routinely detected in one-dimensional separation of Cd^{2+}-induced HK-2(MT3) cytosol. A trace amount of unmodified MT-1E was observed once, but not for any of the other MTs. Unacetylated N-terminal MT peptides were separated from the acetylated forms at the SCX step and therefore were not factored into quantitation.

As much as 40% of the total ion signal for a given N-terminal MT peptide was in the methionine sulfoxide form, observed as 16-Da increases in mass and hydrophilic shifts during RP-HPLC (Fig. 2*A*). This is considered a high degree of oxidation based on a recent quantitative proteomic study of

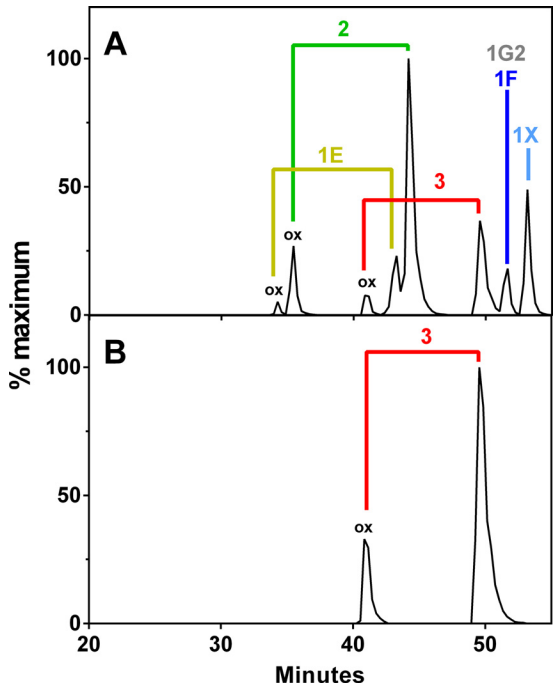

FIG. 2. **Metallothionein N-terminal peptides are susceptible to methionine oxidation.** Cytosol from untreated HK-2(MT3) cells (800 μg) was alkylated with ^{14}N-iodoacetamide. An internal standard of 206 pmol ^{15}N-MT-3 peptide was added. The cytosol was digested with trypsin. The MT peptides were enriched via two-dimensional liquid chromatography followed by MALDI-TOF mass spectrometry as described under "Experimental Procedures," except without the dimethyl sulfide reduction step. *A*, extracted ion chromatogram from 2000 to 2800 *m/z* less the ion intensities of the oxidized and unoxidized MT-3 internal standard. Ion intensities contributed by the N-terminal MT peptides dominate this region. Peaks associated with individual isoforms and their oxidized (ox) forms are annotated accordingly. The maximum peak intensity was 3.1×10^5. *B*, combined extracted ion chromatograms of the ^{15}N-MT-3 internal standard (2423.63 $\pm$ 0.1 *m/z*) and its oxidized form (2439.78 $\pm$ 0.1 *m/z*). The maximum peak intensity was 3.2×10^5.

intracellular methionine oxidation in human Jurkat cells (45). Though N-terminal MT peptides were not detected by the authors, the acetyl-Met-Asp-Pro sequence of MT N termini would classify it as highly susceptible to oxidation based on sequence preferences revealed by this study. The susceptibility of these peptides to oxidation was reinforced by the observation that the addition of synthetic MT peptides to cytosol led to a similar degree of oxidation as in the corresponding endogenous peptides (Fig. 2*B*). This oxidation appeared to occur before the chromatography steps. Further experiments are needed to determine whether methionine oxidation of MTs occurs *in vivo* or is a sample handling artifact.

For purposes of quantitation, it was important to control for the potential variability of methionine oxidation in MTs. Dimethyl sulfide is effective in reversing this modification (42, 46). Fig. 3 illustrates this with the purified, alkylated MT3 N-terminal peptide. Oxidation of the peptide with hydrogen

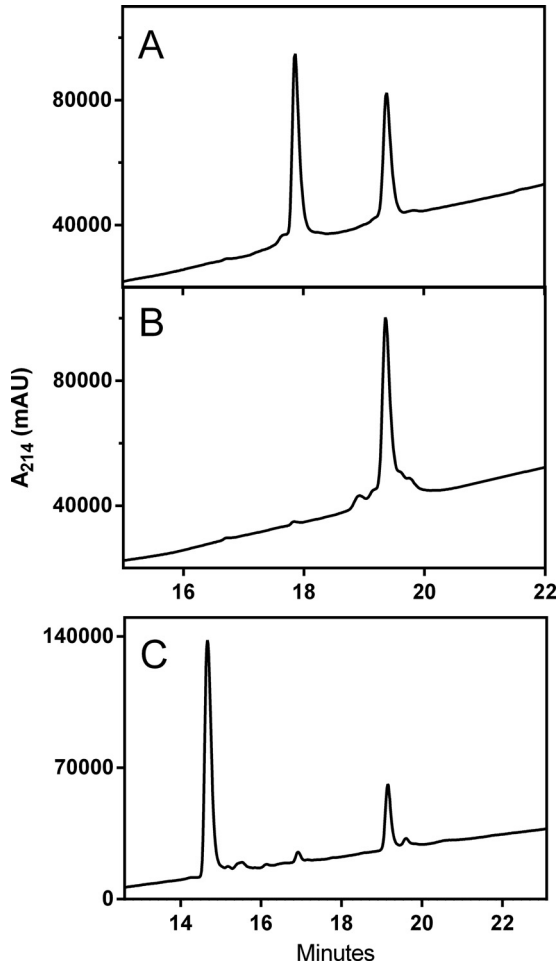

FIG. 3. **Reversible oxidation and acid cleavage of acetylated N-terminal MT peptides.** Purified, carbamidomethylated, acetylated MT-3 peptide was subjected to the indicated chemical treatment and then separated via RP-HPLC as described for peptide purification under "Experimental Procedures," except the gradient was for one hour from 0% to 60% acetonitrile, 0.1% formic acid. Under these conditions the native peptide elutes at about 19 min and the oxidized peptide elutes at about 18 min. Peptide truncated at the Asp-Pro bond elutes before the oxidized form. Peptide treatment before chromatography: (*A*) 30 min at 30 °C in 0.1% hydrogen peroxide, 1% acetic acid; (*B*) oxidized peptide in *A* was incubated for 30 min at room temperature in 0.5 M dimethyl sulfide and 8N HCl as described under "Experimental Procedures"; and (*C*) unoxidized peptide was incubated for 30 min at 100 °C in 0.1% formic acid.

peroxide caused a hydrophilic shift in RP-HPLC (Fig. 3*A*). The hydrophilic status reverted to that of the unoxidized form after dimethyl sulfide treatment (Fig. 3*B*), collapsing the split signal in Fig. 3*A* to a single precursor ion.

In addition to acetylation and oxidation, early experiments showed some truncations of N-terminal peptides, most notably the loss of acetyl-Met-Asp (not shown). The Asp-Pro peptide bonds at the 2–3 position in MTs (47) and in other proteins (48) are acid labile. This susceptibility to cleavage might explain in part why multiple N-terminal MT truncations are observed in the PeptideAtlas database (49, 50). Stoichiometric Asp-Pro cleavage of equine renal MT is achieved with 70% formic acid for 96 h at 40 °C. In contrast, incubation of rat liver MT in 70% formic acid for as much as 70 h at 23 °C does not cause Asp-Pro cleavage (51). We found that extended incubation at 4 °C in 0.1% formic acid or brief heating in inadequately buffered conditions was sufficient to generate detectable truncated N-terminal MT peptides (see supplemental Fig. S4 for an example). The susceptibility of these peptides to cleavage was confirmed by incubating the purified MT-3 peptide for 30 min at 100 °C in 0.1% formic acid, which was sufficient to convert most of the peptide to the truncated form (Fig. 3*C*). The acidic conditions required for methionine sulfoxide reduction did not cause perceptible Asp-Pro bond cleavage (Fig. 3*B*). As a result of these observations, extra precautions were taken to minimize exposure of the samples to low pH and elevated temperature.

Validation of ^{14}N- and ^{15}N-iodoacetamide for Quantitation of N-terminal MT Peptides—The enhanced sensitivity gained with two-dimensional LC and the simplification of precursor ion complexity with dimethyl sulfide treatment were critical for accurate quantitative profiling of MT isoforms. We selected ^{15}N-iodoacetamide as a stable isotope-labeled alkylating agent because it is commercially available, gives a cumulative mass shift of 5 Da for N-terminal MT peptides, and is well characterized for its cysteine-specific reactivity in peptides. This reagent has not been widely used in typical stable isotope labeling experiments because a single Dalton mass shift would complicate quantitation due to the high degree of isotopic envelope overlap. The suitability of ^{15}N-iodoacetamide for the quantitation of MT peptides was evaluated. Extracted ion chromatograms of equimolar mixtures of endogenous ^{14}N- and ^{15}N-labeled N-terminal MT peptides from Cd^{2+}-induced HK-2(MT3) cells (Fig. 4) showed no chromatographic effects due to isotope labeling for any of the peptides. These properties were recapitulated with ^{14}N-labeled cytosol containing ^{15}N-labeled reference peptides (not shown). The assay was linear over 2 orders of magnitude (Fig. 5). Combined, these results indicate that the optimized MT peptide quantitation strategy is sensitive and reproducible over a wide dynamic range.

A representative experiment in which ^{15}N-labeled MT reference peptides were used for quantitation is illustrated in Fig. 6. As in Fig. 2*A*, the MT peptides dominated the early-eluting portion of the gradient in the mass range above 1910 *m/z* (Fig. 6*A*). Peptide mass fingerprints of peak fractions for each MT peptide (Fig. 6*B*) indicate that with the exception of MT-1G2, non-targeted precursors did not interfere with quantitation. Expanded peptide mass fingerprints (1910 to 2710 *m/z*) of the peak MT fractions further reinforce the conclusion that MT N-terminal peptides dominate this chromatographic and *m/z* region (supplemental Fig. S5). The high quality of spectra was consistently maintained throughout all biological replicates for the HK-2 and breast epithelial cell lines that were examined.

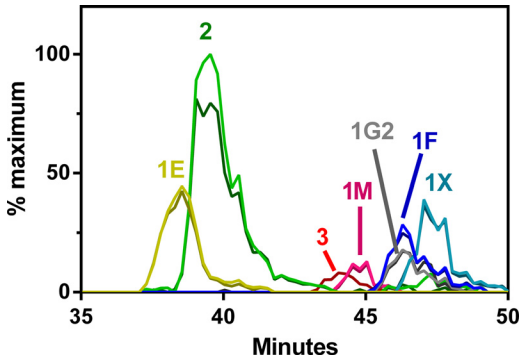

FIG. 4. **The ^{14}N- and ^{15}N-labeled N-terminal MT peptides have similar chromatographic and ionization properties.** Equal amounts of cytosols from Cd^{2+}-induced HK-2(MT3) cells were alkylated with ^{14}N- or ^{15}N-iodoacetamide, combined, and digested with trypsin. The N-terminal MT peptides were enriched as described under "Experimental Procedures" and analyzed via MALDI-TOF/TOF-MS. Extracted ion chromatograms for each MT peptide were based on the observed MH^{1+} monoisotopic mass ± 0.1 *m/z*. Isoforms are color-coded as follows: MT-1E, yellow; MT-1F, green; MT-1G2, gray; MT-1M, magenta; MT-1X, cyan; MT-2, blue; and MT-3, red. The lighter shaded lines are ^{14}N-labeled peptides. The mostly hidden co-elution darker shaded lines are the corresponding ^{15}N-labeled MT peptides. The maximum peak intensity was 1×10^6.

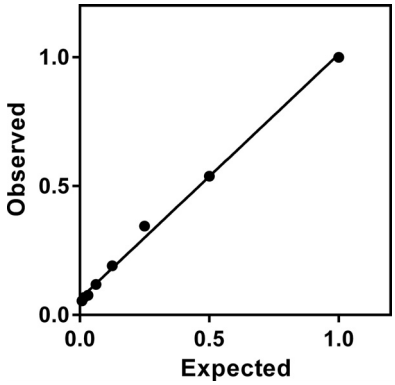

FIG. 5. **Sensitivity and dynamic range of MT-2.** A 2-fold serial dilution of ^{14}N-labeled HK-2(MT3) cytosol was mixed with a constant amount of ^{15}N-labeled cytosol and the samples were digested, fractionated, and analyzed as described under "Experimental Procedures." A 1:1 correlation was observed for observed *versus* calculated ^{14}N/^{15}N MT-2 ratios over 2 orders of magnitude ($r^2 = 0.996$). The signal-to-noise ratio for these samples ranged from 3 to 109.

Commercially available $^{13}C_2$-iodoacetic acid was also evaluated for its suitability for quantitative analysis of MT peptides. This compound gave a cumulative mass shift of 10 Da, and no isotope effects were observed (not shown). The increased hydrophilicity introduced by the carboxylates weakened their retention during RP-HPLC sufficiently to compromise reproducible quantitation.

Quantitation of MT mRNA and Protein Expression in Cd^{2+}-exposed HK-2(MT3) Cells—MTs in the kidney, in particular in the proximal tubule epithelia, are highly responsive to Cd^{2+} exposure. Consequently, there has been much effort to evaluate kidney MTs as potential biomarkers for heavy metal toxicity. The immortalized HK-2 human proximal epithelial cell line is a convenient model for studying proximal tubule cell function (52). In contrast to human proximal tubule cells, HK-2 cells have lost expression of MT-3 (53). Restoration of this gene causes the cells to dome and exhibit vectorial active transport similar to human proximal tubule cells grown in culture (38). The MT mRNA expression of human proximal tubule cells has been qualitatively evaluated via RT-PCR (19, 54, 55) and Northern blot analysis (56, 57). Combined, these studies paint a broad picture of MT isoform mRNA expression of MT-3, MT-2A, MT-1A, MT-1E, MT-1F, and MT-1X, and possibly of MT-1G. Of these, at least MT-1A and MT-1E are induced by Cd^{2+} exposure. In these same studies, protein expression was determined based on immunohistochemistry and dot blot Westerns using the E9 antibody. The MT-1/2 protein expression was induced at least 30-fold upon 3 days of exposure to Cd^{2+}. The quantitation of individual MT isoforms and their induction at the protein level by Cd^{2+} has not yet been described. Real-time quantitative PCR and the mass-spectrometry-based MT isoform assay were applied to this model system to provide a higher resolution, more quantitative assessment of MT expression in this cell type. The use of the HK-2 cell line stably transfected with MT-3 (HK-2(MT3)) provided further opportunity to compare the cytomegalovirus (CMV) promoter-driven MT-3 gene expression, designed for high-efficiency protein expression, with the endogenous MT-1 and MT-2 counterparts.

The mRNA expression of human MT isoforms in HK-2(MT3) cells was determined via real-time quantitative PCR (Fig. 7*A*, supplemental Table S2). These results are consistent with previous analyses of human proximal tubule cells with respect to MT-1E and MT-2 being the most abundant species. Unlike in previous studies, MT-1A was not observed. Of the seven isoforms detected in this study, MT-1M was previously unreported for HK-2 cells.

The absolute protein abundance of individual MT isoforms was determined in HK-2(MT3) cells using the ^{15}N-labeled synthetic MT peptides as internal standards. A mixture containing the seven N-terminal MT peptides observed in HK-2(MT3) cells was added to cytosols that had been alkylated with ^{14}N-iodoacetamide. The spiked cytosols were then trypsin-digested and the N-terminal MT peptides were enriched and analyzed as above. MT isoforms were quantified for both uninduced and Cd^{2+}-induced cells (Fig. 7*B*, supplemental Table S3). The 300 μg of total cytosolic protein used for each experiment was equivalent to the cytosolic protein content of ~3.7×10^6 cells. Assuming a volume of 0.1 pl per cell, the intracellular concentration for MT isoforms ranged from 0.03 mM for MT-1F in uninduced cells to 2 mM for MT-2 in Cd^{2+}-induced cells (0.11 to 7.28 ng per μg total protein, or 1.8 to 120 million copies per cell, respectively). The six MTs detected in the uninduced cells accounted for 0.33% of total protein, whereas the seven MTs detected in Cd^{2+}-induced cells accounted for 1.46% of the total cytosolic protein. At 1.8

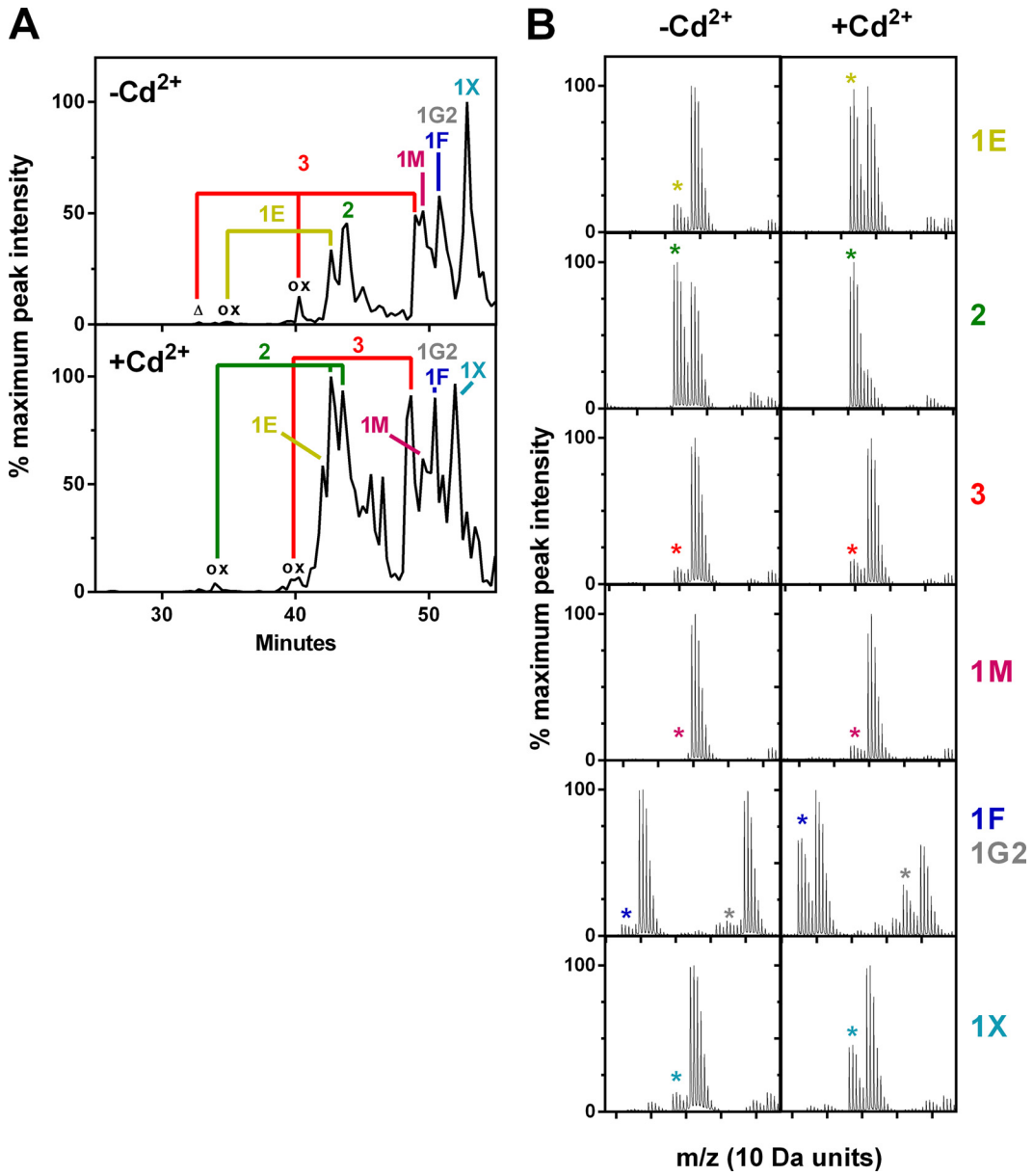

FIG. 6. **Absolute quantitation of N-terminal MT peptides in HK-2(MT3) cells using ^{15}N-labeled reference peptides.** Confluent domed HK-2(MT3) cells were maintained for 3 days in the absence or presence of 9 μM Cd^{2+}. Cytosols were prepared and analyzed as described under "Experimental Procedures." Briefly, 300 μg of each were reduced and alkylated with ^{14}N-iodoacetamide and ^{15}N-labeled MT reference peptides were added. Samples were trypsin-digested and MT peptides were enriched via two-dimensional liquid chromatography. Methionine oxidation was reversed by dimethyl sulfide treatment. Peptides were analyzed via MALDI-TOF/TOF-MS. *A*, extracted ion chromatograms (1910 to 2710 *m/z*) for samples from untreated and Cd^{2+}-treated cells. Low levels of some oxidized MT peptides (ox) were still detectable even after dimethyl sulfide treatment. Very low levels of MT-3 peptide cleaved at the Asp-Pro bond (Δ) were also observed. Observed oxidized and truncated products are linked to their parent peptides with brackets. The maximum peak intensity was 1.9×10^6 and 3.4×10^5 for untreated and Cd^{2+}-treated cells, respectively. *B*, peptide mass fingerprints of each MT peptide from *A* showing a 50 Da region centered on the *m/z* of the ^{15}N-labeled reference peptide (see Table I for individual masses). See supplemental Fig. S5 for expanded versions for each of these MS spectra. Individual isoforms are designated by colors as in Fig. 4. The isotopic envelope of each ^{14}N-labeled MT peptide is indicated (*).

to 120 million copies per cell, all detected MT isoforms qualify as high-abundance proteins based on criteria described by Beck and colleagues (58).

The fold induction determined by the absolute quantitation method was comparable to values measured by the relative method in which equal parts of cytosol from ^{14}N-labeled uninduced and ^{15}N-labeled Cd^{2+}-induced cells were combined and analyzed (Table II). The MT-1F isoform showed the highest induction at 12-fold. The MT-3 isoform, under the control of the CMV promoter (38) which is not responsive to metals, was induced only 1.7-fold. The lack of detection of MT-1M protein in uninduced HK-2(MT3) cells

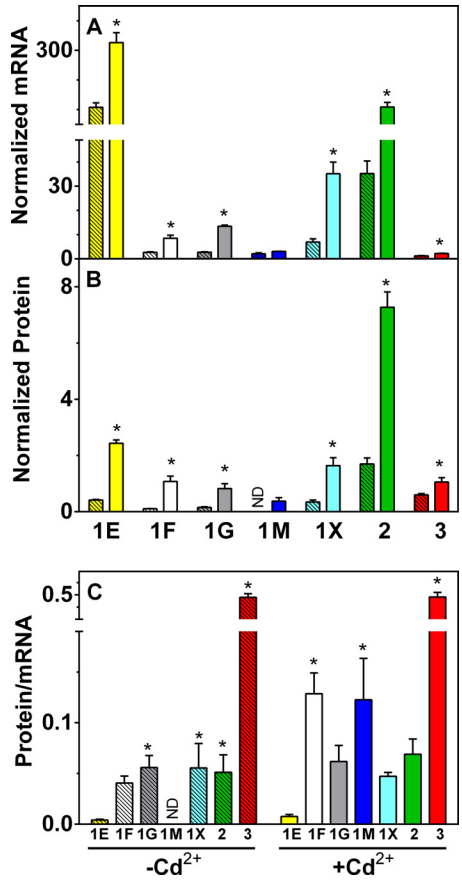

FIG. 7. **mRNA and protein expression of MT isoforms in HK-2(MT3) Cells.** Confluent, domed HK-2(MT3) cells were maintained for 3 days in the absence (hatched bars) or presence (solid bars) of 9 μM Cd^{2+}. Individual isoforms are designated by colors as in Fig. 4. *A*, MT isoform mRNA expression was determined via real-time quantitative PCR and normalized to 1×10^6 18S rRNA transcripts. *B*, MT isoform protein expression was determined from data like those shown in Fig. 6. Absolute quantitation was as described under "Experimental Procedures." Values were normalized to 1 μg of cytosolic protein. The control and treated values for each isoform in *A* and *B* were subjected to a two-tailed unpaired *t* test followed by Tukey's post-test (*$p < 0.05$). *C*, ratios of protein and mRNA were determined from the same biological replicates shown in *A* and *B*. One-way analysis of variance followed by Tukey's post-test was done independently for the $-Cd^{2+}$- and $+Cd^{2+}$-treated cells. The protein/mRNA ratios of isoforms that were significantly different from MT-1E are indicated with an asterisk (*$p < 0.05$). All experiments represent the mean and standard deviation of three independent biological replicates.

suggests that MT-1M may be present but at levels below the detection threshold of the mass-spectrometry-based assay.

The quantitative PCR and mass spectrometric analysis described above permitted comparisons of protein-to-mRNA ratios across MT isoforms. The relative order of MT isoform abundance differed between mRNA and protein expression. For example, MT-1E mRNA was the most abundant, whereas MT-2 protein levels were greatest (compare Figs. 7*A* and 7*B*).

TABLE II

Fold-induction of MT isoform mRNA and protein expression in Cd^{2+}-exposed HK-2(MT3) cells. The mRNA values were calculated from quantitative PCR data (see supplemental Table S2 and Fig. 7A). Protein induction was calculated from mass spectrometry data using the absolute (supplemental Table S3 and Fig. 7B) and relative (not shown) quantitation methods. The fold induction of MT-1M could not be calculated because it was not detectable in uninduced cells. Values are the mean of three biological replicates ± standard deviation. Protein values for a given isoform that are significantly different from the corresponding mRNA value are indicated ($p < 0.05$) as determined by one-way analysis of variance followed by a Tukey's post-test*

Isoform	mRNA	Protein	
		Relative	Absolute
MT-1E	3.1 ± 0.4	6.2 ± 1.1*	5.9 ± 0.5*
MT-1F	3.1 ± 0.4	12.0 ± 2.8*	9.9 ± 1.9*
MT-1G2	5.0 ± 0.6	5.2 ± 0.5	5.4 ± 1.3
MT-1M	1.6 ± 0.5	-	-
MT-1X	5.2 ± 0.4	5.6 ± 0.9	4.7 ± 1.8
MT-2	3.2 ± 0.9	4.8 ± 1.1	4.3 ± 0.9
MT-3	1.7 ± 0.1	1.7 ± 0.1	1.8 ± 0.2

Fig. 7*C* shows the protein/mRNA ratios of each MT isoform. The protein/mRNA ratio for MT-1E was one-tenth that of MT-2. In contrast, the ratios for MT-1X, MT-1G2, MT-1F, and MT-1M were within 2-fold of each other whether determined from Cd^{2+}-induced or uninduced cells. Recombinant MT-3, which is driven by a promoter designed to maximize protein expression, has a protein/mRNA ratio that is at least 7-fold greater than that of any other isoform. Collectively, these results suggest that MT-1E protein expression is less efficient than that of other endogenous MT isoforms, and that as a class MT isoforms demonstrate protein expression efficiency that is markedly less than that of the protein-expression-optimized recombinant MT-3.

Quantitation of MT Isoforms in Human Breast Epithelial Cancer Cells—Previous studies demonstrated that the expression of MT mRNA was limited to MT-2, MT-1E, and MT-1X in human breast ductal epithelia and spontaneously immortalized and cancer cell lines derived from human breast epithelia (26, 41). Cancer cell lines were further distinguished by the much higher expression of these isoforms in ER^- cells than in ER^+ cells (26). Antibody-based methods showed a similar increase in general MT-1/2 protein expression. The mRNA and protein measurements in these studies were semi-quantitative. This model system was selected as a test case to quantitatively compare MT isoform-specific mRNA and protein expression.

Quantitative real-time PCR showed that mRNA expression was limited to MT-2, MT-1E, and MT-1X in the ER^- Hs578T and MDA-MB-231 cancer cell lines and in the spontaneously immortalized nontumorigenic MCF-10A cell line, whereas only MT-2 and MT-1X were detected in the ER^+ MCF-7 and T47D cell lines (Fig. 8, left-hand panels; supplemental Table S4). The ER^- cell lines had characteristically more MT mRNA

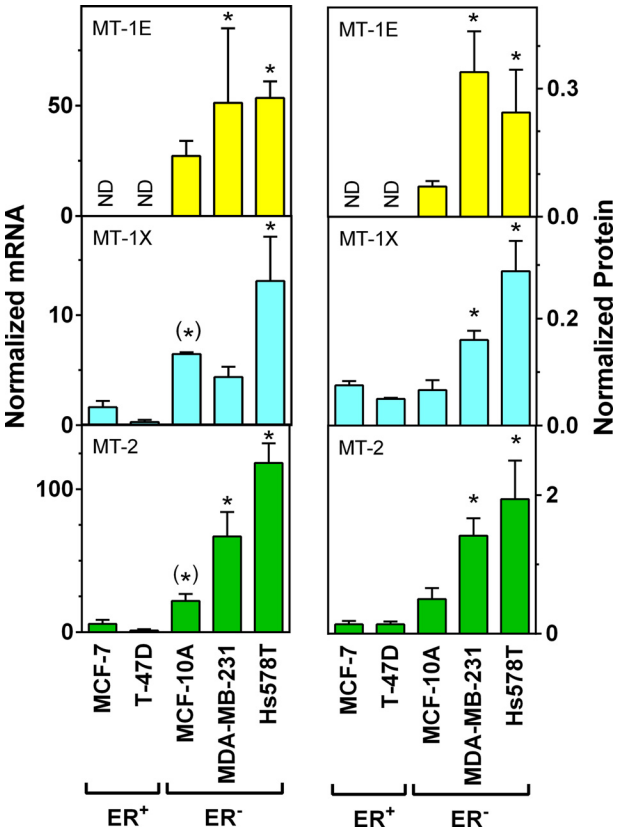

FIG. 8. **mRNA and protein expression of MT isoforms in human breast epithelial cell lines.** MT isoform mRNA (left-hand panels) and protein (right-hand panels) expression was determined as described for Fig. 7. The ER^+ (MCF-7 and T-47D) and ER^- (MCF-10A, MDA-MB-231, and Hs578T) cell lines were cultured and harvested as described under "Experimental Procedures." All experiments represent the mean and standard deviation of three independent biological replicates. Statistical significance ($*p < 0.05$) between either MCF-7 or T-47D cells and any of the ER^- cell lines was determined via one-way analysis of variance followed by a Tukey's post-test. Asterisks in parentheses indicate that the significance applies only to comparison with the T-47D cell line.

expression than their ER^+ counterparts. These general observations are consistent with the previously published qualitative data on the same cell lines (26, 41). Transcript levels in the current study spanned a 400-fold dynamic range.

Preliminary screening for N-terminal MT peptides via mass spectrometry revealed the same complement of MT isoforms identified at the mRNA level, including the restriction of MT-1E expression to ER^- cell lines. These isoforms were quantified using ^{15}N-labeled MT-2, MT-1E, and MT-1X peptides as internal standards (Fig. 8, right-hand panels; supplemental Table S5). The dynamic range of individual MT isoform expression was 38-fold. The dynamic range of total MT isoform expression was 13-fold. This is seven times greater than the 1.8-fold dynamic range in MT-1/2 expression observed earlier with antibody-based methods (26).

The MT-1E isoform represents 30% to 50% of all MT transcripts but only 10% to 18% of all MT protein in ER^- cell lines. This appears to be due primarily to an MT-1E protein/mRNA ratio 4- to 6-fold less than that of either MT-1X or to MT-2 (not shown). In conclusion, MT-1E is not detectable in ER^+ cells at either the mRNA or the protein level, but it is actively transcribed and translated in ER^- cells. The expression efficiency of MT-1E protein relative to mRNA, however, is reduced relative to the two other MT isoforms that are expressed in all breast cancer cell lines tested.

DISCUSSION

The special properties of human MT isoforms present challenges that until now have prevented their accurate characterization at the protein level in complex biological samples. This includes their small size, high cysteine content, highly conserved structure, and large number of isoforms. Antibody-based methods have been routinely used to quantify MT expression in tissues, but the limited specificity of reagents and the potential influence of post-translational modifications upon antigen recognition, physiological or otherwise, compromise the effectiveness of this approach. There is sufficient divergence of the 5′ and 3′ untranslated regions of the MT mRNAs to quantify isoform-specific transcripts, and many PCR-based studies have demonstrated their differential expression in a variety of normal, diseased, or environmentally insulted tissues and cell lines. These changes, however, might not always reflect a one-to-one correlation with protein expression. The mass-spectrometry-based method described in this study addresses many of these challenges.

Detection of MT peptides, especially the critical N-terminal peptides, appears to be sporadic in global proteomic profiling studies. A survey of the Human 2012–10-11 build of the PeptideAtlas database (47, 48) reveals that N-terminal MT peptides are identified in only 10 of 467 samples in the repository. Seven of these datasets have been published (58–62). Combined, these studies identified only three MT N-terminal peptides (MT-2, MT-1E, and MT-1X). Only one study detected the acetylated forms of MT-1X and MT-1E (62). The rest detected only unacetylated forms because N-terminal protein acetylation was not selected as a variable modification for database searches.

Even when N-terminal acetylated proteins are specifically targeted for profiling, the detection of MT peptides is still limited to the abundant MT-2 and MT-1X (63). The COFRADIC approach, which has been successfully applied to the mass spectrometric characterization of many blocked N termini (64, 65), excludes acetylated N-terminal MT peptides because the method requires cleavage at arginine residues, which are absent from all human MTs except MT-4.

Because human MT isoforms are distinguished by only one to three tryptic peptides, the label-free methods utilized in the two PeptideAtlas-referenced studies that reported MT abundance (58, 62) are not sufficiently robust for their accurate quantitation even if N-terminal acetylated peptides are mea-

sured. Accurate quantitation is further compromised in global studies that do not incorporate N-terminal acetylation into their search parameters. One can conclude from this survey that most global proteomic profiling strategies are not optimized for MT quantitation and might even yield misleading results.

As reported previously (34) and described in detail here, the only MT peptide that distinguishes all isoforms is the N-terminal tryptic peptide. Because of this, the question of N-terminal acetylation is a critical one for MT quantitation. Edman sequencing of several mammalian MTs in the 1970s and 1980s demonstrated that the N-terminal methionine was acetylated (46, 65–67). This conclusion is consistent with more recent general studies of N termini that show that proteins beginning with Met-Asp, such as human MTs, are almost completely acetylated (63, 65, 68). Other studies utilizing capillary electrophoresis and mass spectrometry detected trace amounts of unacetylated MTs (69–72). The fraction of unacetylated MT-2 reached 20% in livers of zinc-treated rats (70). Unacetylated MT might have physiological relevance, as its metal-binding properties are distinct from those of the acetylated form (71). MTs are likely stoichiometrically N-acetylated except under metal-stressed conditions, when a minor degree of under-acetylation may be observed. Our results are consistent with near-stoichiometric acetylation of all MT isoforms, even in metal-induced cells.

Until this study, the extent of the problem of N-terminal methionine oxidation was not appreciated for MTs. This has serious implications for the quantitation of MT isoforms. Structural studies of MTs based on Edman sequencing or amino acid analysis (46, 51, 66, 67) were not designed to detect the oxidation state of this residue. In all cases the acetylated methionine was removed to unblock the N terminus by means of either cyanogen bromide cleavage (51, 66, 67) or acid cleavage of the Asp-Pro bond at the 2–3 position (46). These methods utilized acidic conditions that favor the reversion of methionine sulfoxide to methionine (73, 74). It is unknown whether oxidized methionine compromises quantitation utilizing anti-MT antibodies that recognize the five most N-terminal residues, including the acetylated methionine, in MT isoforms (29–31). The dimethyl sulfide treatment used in this study eliminated this problem by converting methionine sulfoxides back to methionine.

Reliance on a single distinguishing peptide to identify and quantify the complement of human MT isoforms required the development of a chemical labeling strategy that targeted this peptide. We exploited the unusually high cysteine content of the N-terminal MT peptides to introduce mass tags via isotopically labeled alkylating agents for quantitative profiling, an approach first described in 1998 using deuterated acrylamide (75) and later popularized with the iodoacetamide-based isotopic-coded affinity tag (ICAT) method of quantitative analysis (76). Very few tryptic peptides contain five cysteines. Labeling of MT peptides with ^{15}N iodoacetamide created a distinctive 5-Da mass shift relative to ^{14}N labeling, making them readily distinguishable from the bulk of peptides. Amplification of isotope effects is a potential disadvantage for high-density labeling. This phenomenon has been observed for some isotopically labeled alkylating agents (77–79). We observed no isotope effect on MT peptides with ^{15}N- *versus* ^{14}N-carbamidomethylation. Chromatographically silent peptide labeling ensures the most accurate quantitation using reference peptides. This might be a particular concern caused by spot-to-spot variability in signal intensity that can occur with MALDI. This labeling and quantitation strategy is not limited to MALDI-TOF/TOF instruments as described here and should be applicable to any LC-MS/MS system, including electrospray ionization platforms.

Human MT isoforms may be amenable to quantitation via selected reaction monitoring. MS/MS of N-terminal MT peptides indicates that each contains appropriate diagnostic fragment ion transitions, and we demonstrate the feasibility of making peptide standards for quantitation. One caveat is that selected reaction monitoring relies on multiple proteotypic peptides in order for each protein to be quantified, which is not possible for the MT family of proteins. Secondly, one rarely sees N-terminal acetylated peptides as proteotypic peptides, probably because this class of peptides tends to be less strongly ionized than internal tryptic peptides. Any selected reaction monitoring approach would likely need to utilize optimized enrichment conditions and the labeled peptide standards described here in order to have adequate sensitivity and reproducibility for quantitation of this class of proteins.

An important finding of this study is that MT mRNA and protein expression levels are not concordant. It is possible that this could be due to the differential stability of mRNAs relative to protein, though half-life measurements of human MT isoform mRNAs have not been done. Alternatively, each MT isoform may have a distinct protein half-life. The influence of metal binding on MT stabilization and proteolytic susceptibility must also be considered because it has been shown that MTs bound to Cd^{2+} are significantly more protected from degradation (29, 31) and proteolytic cleavage (30, 80, 81). This latter phenomenon is unlikely to explain the results seen here because the protein/mRNA ratios do not change appreciably between Cd^{2+}-treated and untreated cells. One last possibility is that technical limitations associated with the quantitation of peptide standards might be partly responsible for these differences. We attempted to minimize this possibility, but the limiting amounts of ^{15}N-labeled peptide standards prevented independent elemental analysis.

Reduced translational efficiency of MT-1E mRNA is a plausible biological explanation for its low protein/mRNA ratio relative to other MT isoforms. The 5′-untranslated region of MT-1E mRNA is unique among human MT isoforms in that it contains a stable 12-bp GC-rich stem-loop structure positioned 26 bases from its 5′ cap. The stability of the stem loop

and its location are consistent with reduced translation efficiency (82). No other MT mRNA has a similar predicted stem-loop as stable as that of MT-1E. Further experiments will be needed to test this hypothesis.

This study also highlights the power of mass spectrometry to detect less abundant forms of MT in human cells. Thus, this study reveals that MT-1M, MT-1F, and MT-1G2 are significant players in metal metabolism along with the more abundant MT-2, MT-1X, and MT-1E in human HK-2 kidney cells.

The discriminating power of mass spectrometry further extends our understanding of MT alternative splice isoforms. Even with the limited number of cell lines and tissues surveyed in this study, it is apparent that the splicing pattern of MT-1G is non-random. MT-1G1 differs from MT-1G2 by the insertion of a single Ala residue at the 3′ splice junction of its first intron. This conditional codon insertion is driven by a NAGNAG alternative splice site (83, 84). Deep RNA sequencing analysis classifies the NAGNAG alternative splicing of MT-1G1/MT-1G2 as highly regulated (84). This single codon differentiation of splice isoforms has not been previously reported in MT expression studies that rely on standard quantitative PCR measurements. Of particular interest is the absence of MT-1G1 in immortalized HK-2 proximal tubule cells, whereas kidney cortex expresses both forms. This suggests that MT-1G1/MT-1G2 ratios may serve as a specific indicator of changes in splicing factors that may be associated with disease states.

In conclusion, this study demonstrates the feasibility of quantifying individual MT isoforms in human cells and tissues at the protein level. The findings are generally consistent with previous studies using human breast and kidney cell lines. The proteomic analysis complements that of mRNA expression by taking into account post-translational modifications, differences in protein expression efficiency, and alternative splicing. This lays the groundwork for the evaluation of MT isoforms as prognostic protein biomarkers in breast cancers and other pathologies. The methodology has potential for application in prospective analyses of tissue biopsies, plasma, or urine and retrospective analysis of formalin-fixed paraffin-embedded tissues.

Acknowledgments—We thank William M. Old, University of Colorado at Boulder, for constructive feedback and critical reading of the manuscript.

* This project was supported by INBRE grants to D.A.S. from the National Center for Research Resources (P20 RR016471) and NIGMS (P20 GM103442), National Institutes of Health. A.A.M. was supported with a North Dakota EPSCoR predoctoral fellowship through a grant from the National Science Foundation (EPS-0814442).

S This article contains supplemental material.

‖ To whom correspondence should be addressed: Tel.: 1-701-777-4946; Fax: 1-701-777-2382; E-mail: john.shabb@med.und.edu.

¶ Current address: Department of Pharmacology and Toxicology, University of Arizona College of Pharmacy, 1295 North Martin, Tucson, AZ 85721.

REFERENCES

1. Hamer, D. H. (1986) Metallothionein. *Annu. Rev. Biochem.* **55,** 913–951
2. Vallee, B. L. (1995) The function of metallothionein. *Neurochem. Int.* **27,** 23–33
3. Vašák, M., and Meloni, G. (2011) Chemistry and biology of mammalian metallothioneins. *J. Biol. Inorg. Chem.* **16,** 1067–1078
4. Penkowa, M. (2006) Metallothioneins are multipurpose neuroprotectants during brain pathology. *FEBS J.* **273,** 1857–1870
5. Bell, S. G., and Vallee, B. L. (2009) The metallothionein/thionein system, an oxidoreductive metabolic zinc link. *ChemBioChem* **10,** 55–62
6. Manso, Y., Adkard, P. A., Carrasco, J., Vašák, M., and Hidalgo, J. (2011) Metallothionein and brain inflammation. *J. Biol. Inorg. Chem.* **16,** 1103–1113
7. Nordberg, G. F. (2009) Historical perspectives on cadmium toxicology. *Toxicol. Appl. Pharmacol.* **238,** 192–200
8. Mocchegiani, E., Bertoni-Freddari, C., Marcellini, F., and Malavolta, M. (2005) Brain, aging and neurodegeneration: role of zinc ion availability. *Prog. Neurobiol.* **75,** 367–390
9. Cherian, M. G., Jayasurya, A., and Bay, B. H. (2003) Metallothioneins in human tumors and potential roles in carcinogenesis. *Mutat. Res.* **533,** 201–209
10. Pedersen, M. O., Larsen, A., Stoltenberg, M., and Penkowa, M. (2009) The role of metallothionein in oncogenesis and cancer prognosis. *Prog. Histochem. Cytochem.* **44,** 29–64
11. Laukens, D., Waeytens, A., De Bleser, P., Cuvelier, C., and De Vos, M. (2009) Human metallothionein expression under normal and pathological conditions: mechanisms of gene regulation based on *in silico* promoter analysis. *Crit. Rev. Eukaryot. Gene Expr.* **19,** 301–317
12. Martin, J., Han, C., Gordon, L. A., Terry, A., Prabhakar, S., She, X., Xie, G., Hellsten, U., Chan, Y. M., Altherr, M., Couronne, O., Aerts, A., Bajorek, E., Black, S., Blumer, H., Branscomb, E., Brown, N. C., Bruno, W. J., Buckingham, J. M., Callen, D. F., Campbell, C. S., Campbell, M. L., Campbell, E. W., Caoile, C., Challacombe, J. F., Chasteen, L. A., Chertkov, O., Chi, H. C., Christensen, M., Clark, L. M., Cohn, J. D., Denys, M., Detter, J. C., Dickson, M., Dimitrijevic-Bussod, M., Escobar, J., Fawcett, J. J., Flowers, D., Fotopulos, D., Glavina, T., Gomez, M., Gonzales, E., Goodstein, D., Goodwin, L. A., Grady, D. L., Grigoriev, I., Groza, M., Hammon, N., Hawkins, T., Haydu, L., Hildebrand, C. E., Huang, W., Israni, S., Jett, J., Jewett, P. B., Kadner, K., Kimball, H., Kobayashi, A., Krawczyk, M. C., Leyba, T., Longmire, J. L., Lopez, F., Lou, Y., Lowry, S., Ludeman, T., Manohar, C. F., Mark, G. A., McMurray, K. L., Meincke, L. J., Morgan, J., Moyzis, R. K., Mundt, M. O., Munk, A. C., Nandkeshwar, R. D., Pitluck, S., Pollard, M., Predki, P., Parson-Quintana, B., Ramirez, L., Rash, S., Retterer, J., Ricke, D. O., Robinson, D. L., Rodriguez, A., Salamov, A., Saunders, E. H., Scott, D., Shough, T., Stallings, R. L., Stalvey, M., Sutherland, R. D., Tapia, R., Tesmer, J. G., Thayer, N., Thompson, L. S., Tice, H., Torney, D. C., Tran-Gyamfi, M., Tsai, M., Ulanovsky, L. E., Ustaszewska, A., Vo, N., White, P. S., Williams, A. L., Wills, P. L., Wu, J. R., Wu, K., Yang, J., Dejong, P., Bruce, D., Doggett, N. A., Deaven, L., Schmutz, J., Grimwood, J., Richardson, P., Rokhsar, D. S., Eichler, E. E., Gilna, P., Lucas, S. M., Myers, R. M., Rubin, E. M., and Pennacchio, L. A. (2004) The sequence and analysis of duplication-rich human chromosome 16. *Nature* **432,** 988–994
13. Uhlen, M., Oksvold, P., Fagerberg, L., Lundberg, E., Jonasson, K., Forsberg, M., Zwahlen, M., Kampf, C., Wester, K., Hober, S., Wernerus, H., Björling, L., and Ponten, F. (2010) Towards a knowledge-based Human Protein Atlas. *Nat. Biotechnol.* **28,** 1248–1250
14. Uhlén, M., Björling, E., Agaton, C., Szigyarto, C. A., Amini, B., Andersen, E., Andersson, A. C., Angelidou, P., Asplund, A., Asplund, C., Berglund, L., Bergström, K., Brumer, H., Cerjan, D., Ekström, M., Elobeid, A., Eriksson, C., Fagerberg, L., Falk, R., Fall, J., Forsberg, M., Björklund, M. G., Gumbel, K., Halimi, A., Hallin, I., Hamsten, C., Hansson, M., Hedhammar, M., Hercules, G., Kampf, C., Larsson, K., Lindskog, M., Lodewyckx, W., Lund, J., Lundeberg, J., Magnusson, K., Malm, E., Nilsson, P., Odling, J., Oksvold, P., Olsson, I., Oster, E., Ottosson, J., Paavilainen, L., Persson, A., Rimini, R., Rockberg, J., Runeson, M., Sivertsson, A., Sköllermo, A., Steen, J., Stenvall, M., Sterky, F., Strömberg, S., Sundberg, M., Tegel, H., Tourle, S., Wahlund, E., Waldén, A., Wan, J., Wernérus, H., Westberg, J., Wester, K., Wrethagen, U., Xu, L. L., Hober, S., and Pontén, F. (2005) A human protein atlas for normal and cancer tissues based on antibody proteomics. *Mol. Cell. Proteomics* **4,** 1920–1932

15. Schmidt, C. J., and Hamer, D. H. (1986) Cell specificity and effect of ras on human MT gene expression. *Proc. Natl. Acad. Sci. U.S.A.* **83,** 3346–3350
16. Heguy, A., West, A., Richards, R. I., and Karin, M. (1986) Structure and tissue-specific expression of the human metallothionein IB gene. *Mol. Cell. Biol.* **6,** 2149–2157
17. Foster, R., Jahroudi, N., Varshney, U., and Gedamu, L. (1988) Structure and expression of the human metallothionein-IG gene. *J. Biol. Chem.* **263,** 11528–11535
18. Tsuji, S., Kobayashi, H., Uchida, Y., Ihara, Y., and Miyatake, T. (1992) Molecular cloning of human growth inhibitory factor cDNA and its down-regulation in Alzheimer's disease. *EMBO J.* **11,** 4843–4850
19. Hoey, J. G., Garrett, S. H., Sens, M. A., Todd, J. H., and Sens, D. A. (1997) Expression of MT-3 mRNA in human kidney, proximal tubule cell cultures, and renal cell carcinoma. *Toxicol. Lett.* **92,** 149–160
20. Quaife, C. J., Findley, S. D., Erickson, J. C., Froelick, G. J., Kelly, E. J., Zambrowicz, B. P., and Palmiter, R. D. (1994) Induction of a new metallothionein isoform (MT-IV) occurs during differentiation of stratified squamous epithelia. *Biochemistry* **33,** 7250–7259
21. Jin, R., Chow, V. T.-K., Tan, P.-H., Dheen, S. T., Duan, W., and Bay, B.-H. (2002) Metallothionein 2A expression is associated with cell proliferation in breast cancer. *Carcinogenesis* **23,** 81–86
22. Jin, R., Bay, B. H., Chow, V. T. K., and Tan, P. H. (2001) Metallothionein 1F mRNA expression correlates with histological grade in breast carcinoma. *Breast Cancer Res. Treat.* **66,** 265–272
23. Sens, M. A., Somji, S., Garrett, S. H., Beall, C. L., and Sens, D. A. (2001) Metallothionein isoform 3 overexpression is associated with breast cancers having a poor prognosis. *Am. J. Pathol.* **159,** 21–26
24. Somji, S., Garrett, S. H., Zhou, X. D., Zheng, Y., Sens, D. A., and Sens, M. A. (2010) Absence of metallothionein 3 expression in breast cancer is a rare, but favorable marker of outcome that is under epigenetic control. *Toxicol. Environ. Chem.* **92,** 1673–1695
25. Jin, R., Bay, B. H., Chow, V. T. K., Tan, P. H., and Lin, V. C. L. (2000) Metallothionein 1E mRNA is highly expressed in oestrogen receptor-negative human invasive ductal breast cancer. *Br. J. Cancer* **83,** 319–323
26. Friedline, J. A., Garrett, S. H., Somji, S., Todd, J. H., and Sens, D. A. (1998) Differential expression of the MT-1E gene in estrogen-receptor-positive and -negative human breast cancer cell lines. *Am. J. Pathol.* **152,** 23–27
27. Garrett, S. H., Sens, M. A., Todd, J. H., Somji, S., and Sens, D. A. (1999) Expression of MT-3 protein in the human kidney. *Toxicol. Lett.* **105,** 207–214
28. Jasani, B., and Schmid, K. W. (1997) Significance of metallothionein overexpression in human tumours. *Histopathology* **31,** 211–214
29. Cousins, R. J. (1979) Metallothionein synthesis and degradation: relationship to cadmium metabolism. *Environ. Health Perspect.* **28,** 131–136
30. Winge, D. R., and Miklossy, K. A. (1982) Domain nature of metallothionein. *J. Biol. Chem.* **257,** 3471–3476
31. Monia, B. P., Butt, T. R., Ecker, D. J., Mirabelli, C. K., and Crooke, S. T. (1986) Metallothionein turnover in mammalian cells. *J. Biol. Chem.* **261,** 10957–10959
32. Theocharis, S. E., Margeli, A. P., Klijanienko, J. T., and Kouraklis, G. P. (2004) Metallothionein expression in human neoplasia. *Histopathology* **45,** 103–118
33. Namdarghanbari, M., Wobig, W., Krezoski, S., Tabatabai, N. M., and Petering, D. H. (2011) Mammalian metallothionein in toxicology, cancer, and cancer chemotherapy. *J. Biol. Inorg. Chem.* **16,** 1087–1101
34. Wang, R., Sens, D. A., Albrecht, A., Garrett, S., Somji, S., Sens, M. A., and Lu, X. (2007) Simple method for identification for metallothionein isoforms in cultured human prostate cells by MALDI-TOF/TOF mass spectrometry. *Anal. Chem.* **79,** 4433–4441
35. Alvarez, L., Gonzalez-Iglesias, H., Garcia, M., Ghosh, S., Sanz-Medel, A., and Coca-Prados, M. (2012) The stoichiometric transition from Zn_6Cu_1-metallothionein to Zn_7-metallothionein underlies the up-regulation of metallothionein (MT) expression: quantitative analysis of MT-metal load in eye cells. *J. Biol. Chem.* **287,** 28456–28469
36. Mounicou, S., Ouerdane, L., L'Azou, B., Passagne, I., Ohayon-Courtès, C., Szpunar, J., and Lobinski, R. (2010) Identification of metallothionein subisoforms in HPLC using accurate mass and online sequencing by electrospray hybrid linear ion trap-orbital ion trap mass spectrometry. *Anal. Chem.* **82,** 6947–6957
37. Mididoddi, S., McGuirt, J. P., Sens, M. A., Todd, J. H., and Sens, D. A. (1996) Isoform-specific expression of metallothionein mRNA in the developing and adult human kidney. *Toxicol. Lett.* **85,** 17–27
38. Kim, D., Garrett, S. H., Sens, M. A., Somji, S., and Sens, D. A. (2002) Metallothionein isoform 3 and proximal tubule vectorial active transport. *Kidney Int.* **61,** 464–472
39. Somji, S., Garrett, S. H., Sens, M. A., Gurel, V., and Sens, D. A. (2004) Expression of metallothionein isoform 3 (MT-3) determines the choice between apoptotic or necrotic cell death in Cd^{+2}-exposed human proximal tubule cells. *Toxicol. Sci.* **80,** 358–366
40. Gurel, V., Sens, D. A., Somji, S., Garrett, S. H., Nath, J., and Sens, M. A. (2003) Stable transfection and overexpression of metallothionein isoform 3 inhibits the growth of MCF-7 and Hs578T cells but not that of T-47D or MDA-MB-231 cells. *Breast Cancer Res. Treat.* **80,** 181–191
41. Gurel, V., Sens, D. A., Somji, S., Garrett, S. H., Weiland, T., and Sens, M. A. (2005) Post-transcriptional regulation of metallothionein isoform 1 and 2 expression in the human breast and the MCF-10A cell line. *Toxicol. Sci.* **85,** 906–915
42. Shechter, Y. (1986) Selective oxidation and reduction of methionine residues in peptides and proteins by oxygen exchange between sulfoxide and sulfide. *J. Biol. Chem.* **261,** 66–70
43. Somji, S., Garrett, S. H., Sens, M. A., and Sens, D. A. (2006) The unique N-terminal sequence of metallothionein-3 is required to regulate the choice between apoptotic or necrotic cell death of human proximal tubule cells exposed to Cd^{+2}. *Toxicol. Sci.* **90,** 369–376
44. Dormeyer, W., Mohammed, S., van Breukelen, B., Krijgsveld, J., and Heck, A. J. R. (2007) Targeted analysis of protein termini. *J. Proteome Res.* **6,** 4634–4645
45. Ghesquiére, B., Jonkheere, V., Colaert, N., Van Durme, J., Timmerman, E., Goethals, M., Schymkowitz, J., Rousseau, F., Vandekerchkove, J., and Gevaert, K. (2011) Redox proteomics of protein-bound methionine oxidation. *Mol. Cell. Proteomics* **10,** M110.006866
46. Lipton, S. H., and Bodwell, C. E. (1976) Specific oxidation of methionine to methionine sulfoxide. *J. Agric. Food Chem.* **24,** 26–31
47. Kojima, Y., Berger, C., Vallee, B. L., and Kägi, J. H. R. (1976) Amino acid sequence of equine renal metallothionein-1B. *Proc. Natl. Acad. Sci. U.S.A.* **73,** 3413–3417
48. Landon, M. (1977) Cleavage at aspartyl-prolyl bonds. *Methods Enzymol.* **47,** 145–149
49. Desiere, F., Deutsch, E. W., Nesvizhskii, A. I., Mallick, P., King, N. L., Eng, J. K., Aderem, A., Boyle, R., Brunner, E., Donohoe, S., Fausto, N., Hafen, E., Hood, L., Katze, M. G., Kennedy, K. A., Kregenow, F., Lee, H., Lin, B., Martin, D., Ranish, J. A., Rawlings, D. J., Samelson, L. E., Shiio, Y., Watts, J. D., Wollscheid, B., Wright, M. E., Yan, W., Yang, L., Yi, E. C., Zhang, H., and Aebersold, R. (2004) Integration with the human genome of peptide sequences obtained by high-throughput mass spectrometry. *Genome Biol.* **6,** R9
50. Desiere, F., Deutsch, E. W., King, N. L., Nescishskii, A. I., Mallick, P., Eng, J., Chen, S., Eddes, J., Loevenich, S. N., and Aebersold, R. (2006) The PeptideAtlas project. *Nucleic Acids Res.* **34,** D655–D658
51. Winge, D. R., Nielson, K. B., Zeikus, R. D., and Gray, W. R. (1984) Structural characterization of the isoforms of neonatal and adult rat liver metallothionein. *J. Biol. Chem.* **259,** 11419–11425
52. Ryan, M. J., Johnson, G., Kirk, J., Fuerstenberg, S. M., Zager, R. A., and Torok-Storb, B. (1994) HK-2: an immortalized proximal tubule epithelial cell line from normal adult human kidney. *Kidney Int.* **45,** 48–57
53. Garrett, S. H., Phillips, V., Somji, S., Sens, M. A., Dutta, R., Park, S., Kim, D., and Sens, D. A. (2002) Transient induction of metallothionein isoform 3 (MT-3) c-fos, c-jun, and c-myc in human proximal tubule cells exposed to cadmium. *Toxicol. Lett.* **126,** 69–80
54. Garrett, S. H., Somji, S., Todd, J. H., and Sens, D. A. (1998) Exposure of human proximal tubule cells to Cd^{2+}, Zn^{2+}, and Cu^{2+} induces metallothionein protein accumulation but not metallothionein. *Environ. Health Perspect.* **106,** 587–595
55. Garrett, S. H., Somji, S., Todd, J. H., Sens, M. A., and Sens, D. A. (1998) Differential expression of human metallothionein isoform I mRNA in human proximal tubule cells exposed to metals. *Environ. Health Perspect.* **106,** 825–832
56. Bylander, J. E., Li, S. L., Sens, M. A., Hazen-Martin, D., Re, G. G., and Sens, D. A. (1994) Induction of metallothionein mRNA and protein following exposure of cultured human proximal tubule cells to cadmium. *Toxicol. Lett.* **71,** 111–122
57. Bylander, J. E., Li, S. L., Sens, M. A., and Sens, D. A. (1995) Exposure of

human proximal tubule cells to cytotoxic levels of $CdCl_2$ induces the additional expression of metallothionein 1A mRNA. *Toxicol. Lett.* **76,** 209–217
58. Beck, M., Schmidt, A., Malmstroem, J., Claasen, M., Ori, A., Szymborska, A., Herzog, F., Rinner, O., Ellengerg, J., and Aebersold, R. (2011) The quantitative proteome of a human cell line. *Mol. Syst. Biol.* **7,** 549
59. Munoz, J., Low, T. Y., Kok, Y. J., Chin, A., Frese, C. K., Ding, V., Choo, A., and Heck, A. J. R. (2011) The quantitative proteomes of human induced pluripotent stem cells and embryonic stem cells. *Mol. Syst. Biol.* **7,** 550
60. Nagaraj, N., Wisniewski, J. R., Geiger, T., Cox, J., Kircher, M., Kelso, J., Pääbo, S., and Mann, M. (2011) Deep proteome and transcriptome mapping of a human cancer cell line. *Mol. Syst. Biol.* **7,** 548
61. Phanstiel, D. H., Brumbaugh, J., Wenger, C. D., Tian, S., Probasco, M. D., Bailey, D. J., Swaney, D. L., Tervo, M. A., Bolin, J. M., Ruotti, V., Stewart, R., Thomson, J. A., and Coon, J. J. (2011) Proteomic and phosphoproteomic comparison of human ES and iPS cells. *Nat. Methods* **8,** 821–827
62. Geiger, T., Wehner, A., Schaab, C., Cox, J., and Mann, M. (2012) Comparative proteomic analysis of eleven common cell lines reveals ubiquitous but varying expression of most proteins. *Mol. Cell. Proteomics* **11,** M111.014050
63. Helbig, A. O., Gauci, S., Raijmakers, R., van Breukelen, B., Slijper, M., Mohammed, S., and Heck, A. J. R. (2010) Profiling of N-acetylated protein termini provides in-depth insights into the N-terminal nature of the proteome. *Mol. Cell. Proteomics* **9,** 928–939
64. Gevaert, K., Goethals, M., Martens, L., Van Damme, J., Staes, A., Thomas, G. R., and Vandekerckhove, J. (2003) Exploring proteomes and analyzing protein processing by mass spectrometric identification of sorted N-terminal peptides. *Nat. Biotechnol.* **21,** 566–569
65. Arnesen, T., Van Damme, P., Polevoda, B., Helsens, K., Evjenth, R., Colaert, N., Varhaug, J. E., Vandekerckhove, J., Lillehaug, J. R., Sherman, F., and Gevaert, K. (2009) Proteomics analyses reveal the evolutionary conservation and divergence of N-terminal acetyltransferases from yeast and humans. *Proc. Natl. Acad. Sci. U.S.A.* **106,** 8157–8162
66. Huang, I.-Y., Yoshida, A., Tsunoo, H., and Nakajima, H. (1977) Mouse liver metallothioneins: complete amino acid sequence of metallothionein-I. *J. Biol. Chem.* **252,** 8217–8221
67. Huang, I.-Y., Kimura, M., Hata, A., Tsunoo, H., and Yoshida, A. (1981) Complete amino acid sequence of mouse liver metallothionein-II. *J. Biochem.* **89,** 1839–1845
68. Boissel, J.-P., Kasper, T., and Bunn, H. F. (1988) Cotranslational amino-terminal processing of cytosolic proteins: cell-free expression of site-directed mutants of human hemoglobin. *J. Biol. Chem.* **263,** 8443–8449
69. Knudsen, C. B., Bjornsdottir, I., Jons, O., and Hansen, S. H. (1998) Detection of metallothionein isoforms from three different species using on-line capillary electrophoresis-mass spectrometry. *Anal. Biochem.* **265,** 167–175
70. Beattie, J. H., Wood, A. M., and Duncan, G. J. (1999) Rat metallothionein-2 contains N-acetylated and unacetylated forms. *Electrophoresis* **20,** 1613–1618
71. Van Vyncht, G., Bordin, A., and Rodriguez, A. R. (2000) Rabbit liver metallothionein subisoform characterization using liquid chromatography hyphenated to diode array detection and electrospray ionization mass spectrometry. *Chromatographia* **52,** 745–752
72. Andón, B., Barbosa, J., and Sanz-Nebot, V. (2006) Separation and characterization of rabbit liver apothioneins by capillary electrophoresis coupled to electrospray ionization time-of-flight mass spectrometry. *Electrophoresis* **27,** 3661–3670
73. Ray, W. J., and Koshland, D. E. (1962) Identification of amino acids involved in phosphoglucomutase action. *J. Biol. Chem.* **237,** 2493–2505
74. Savige, W. E., and Fontana, A. (1977) Interconversion of methionine and methionine sulfoxide. *Methods Enzymol.* **47,** 453–459
75. Sechi, S., and Chait, B. T. (1998) Modification of cysteine residues by alkylation. A tool in peptide mapping and protein identification. *Anal. Chem.* **70,** 5150–5158
76. Gygi, S. P., Rist, B., Gerber, S. A., Turecek, F., Gelb, M. H., and Aebersold, R. (1999) Quantitative analysis of complex protein mixtures using isotope-coded affinity tags. *Nat. Biotechnol.* **17,** 994–999
77. Zhang, R., and Regnier, F. E. (2002) Minimizing resolution of isotopically coded peptides in comparative proteomics. *J. Proteome Res.* **1,** 139–147
78. Zhang, R., Sioma, C. S., Thompson, R. A., Xiong, L., and Regnier, F. E. (2002) Controlling deuterium isotope effects in comparative proteomics. *Anal. Chem.* **74,** 3662–3669
79. Faca, V., Coram, M., Phanstiel, D., Glukhova, V., Zhang, Q., Fitzgibbon, M., McIntosh, M., and Hanash, S. (2006) Quantitative analysis of acrylamide labeled serum proteins by LC-MS/MS. *J. Proteome Res.* **5,** 2009–2018
80. Nielson, K. B., and Winge, D. R. (1983) Order of metal binding in metallothionein. *J. Biol. Chem.* **258,** 13063–13069
81. Nielson, K. B., Atkin, C. L., and Winge, D. R. (1985) Distinct metal-binding configurations in metallothionein. *J. Biol. Chem.* **260,** 5342–5350
82. Babendure, J. R., Babendure, J. L., Ding, J.-H., and Tsien, R. Y. (2006) Control of mammalian translation by mRNA structure near caps. *RNA* **12,** 851–861
83. Hiller, M., Huse, K., Szafranski, K., Jahn, N., Hampe, J., Schreiber, S., Backhofen, R., and Platzer, M. (2004) Widespread occurrence of alternative splicing at NAGNAG acceptors contributes to proteome plasticity. *Nat. Genet.* **36,** 1255–1257
84. Bradley, R. K., Merkin, J., Lambert, N. J., and Burge, C. B. (2012) Alternative splicing of RNA triplets is often regulated and accelerates proteome evolution. *PLoS Biol.* **10,** e1001229